THE JOURNAL OF PHYSICAL CHEMISTRY B

Article

pubs.acs.org/JPCB

Hydrophobic Collapse of a Stearic Acid Film by Adsorbed L-Phenylalanine at the Air−Water Interface

Elizabeth C. Griffith,[†] Ellen M. Adams,[‡] Heather C. Allen,[‡] and Veronica Vaida*[,†]

[†]Department of Chemistry and Biochemistry and CIRES, University of Colorado at Boulder, UCB 215, Boulder, Colorado 80309, United States

[‡]Department of Chemistry and Biochemistry, The Ohio State University, 100 West 18th Avenue, Columbus, Ohio 43210, United States

Supporting Information

ABSTRACT: The surface morphology of atmospheric aerosol particles can influence the particle's overall effect on climate through enhancing or impeding its ability to uptake and evaporate water. In the work presented here, complementary surface-sensitive information from π−A isotherms, Brewster angle microscopy (BAM), and infrared reflection−absorption spectroscopy (IRRAS) are used to monitor the induced hydrophobic collapse of a surfactant film by an adsorbed amino acid at the air−water interface. The stearic acid film studied here is well-known to form a very stable floating monolayer at the air−water interface, and is shown in this work to withstand isotherm compression−expansion cycles without any premature collapse. With the presence of the water-soluble amino acid L-phenylalanine, however, significant disruption is observed of the stearic acid film, evidenced by the disappearance of its liquid-condensed phase from the isotherm cycles, as well as premature collapse structures observed in the BAM images and a change in intensity in stearic acid's C−H stretching region in the IRRAS spectra. Throughout this process, the surface layer is transformed from a homogeneous hydrophobic surface to an inhomogeneous surface with three-dimensional hydrophobic aggregates as well as hydrophilic "holes" with minimum surfactant coverage.

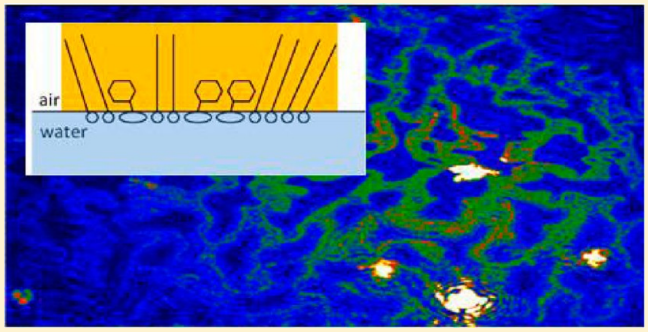

INTRODUCTION

Atmospheric aerosols are globally distributed and are known to play an important role in Earth's atmosphere,[1,2] although their overall effect on climate is difficult to quantify.[3] Organic compounds are ubiquitous components of atmospheric aerosols, recognized to play an important role in climate.[4−6] Aerosols containing organic complex mixtures are either directly emitted or formed by gas-phase photochemistry and adsorbed onto preexisting particles (secondary organic aerosols). Their morphological and chemical properties remain poorly characterized hampering models of their influence on aerosol properties.[7,8] Field measurements have established that many organic compounds found on aerosols in the atmosphere are surface active.[9−13] The morphology and structure of such organic aerosol particles affect their optical properties,[14,15] heterogeneous reaction mechanisms and rates,[16,17] and their ability to form cloud droplets[18−20] and to nucleate ice particles.[21,22]

Due to complex mixtures of hydrophobic and hydrophilic phases in these particles, they can adopt very different structures. Aqueous aerosols, both marine and continental, have been proposed to exist with an inverted micelle structure, with an aqueous core surrounded by a layer of organics.[19,23−25] Recent field observations and laboratory studies find that aerosol particles, in addition to such inverted micelle structures, can adopt other morphologies and contain organic inclusions.[5,26,27] Reid et al. have proposed a complex structure where the organics can form surfactant lenses.[28] The presence of such different phases and structures[29] give rise to different thermodynamic constraints and hence different morphological, optical and chemical properties. The scattering efficiency of aerosol particles has a strong dependency on size,[30] requiring quantitative insight into aerosol size distribution. The composition of the aerosol, especially of the surface, can influence the particle's size through altering its ability to evaporate or absorb water.[8,20,31]

It is commonly accepted that surface films composed of long-chain organics impede water transfer.[25,32−36] This effect is dependent upon the extent of surface coverage and the solubility of the surfactant. The nature of the films formed by soluble versus insoluble surfactants varies: soluble surfactants form more expanded, permeable films, whereas many insoluble surfactants form close-packed, more impermeable films.[25,33,37,38] Environmental interfaces are more complicated

Received: April 23, 2012
Revised: June 11, 2012
Published: June 12, 2012

systems, however, as they contain mixtures of surface active organics. The long-chain fatty acids found on aerosols (such as stearic acid) are insoluble saturated surfactants, and therefore should impede water transfer into and out of the particle, thereby affecting aerosol growth. This idea has been tested experimentally on model aerosol particles in the laboratory, but the results are conflicting.[20,39−42] Moreover, this simplified view relates to one-component monolayers comprised completely of long-chain fully saturated fatty acids. It is likely that both monolayer structure and interfacial water transfer are highly sensitive to both the composition and morphology of the interfacial film. Optical trapping has been used recently to begin to understand some of these complex properties of aerosols (hygroscopicity, mass accommodation, etc.), but it is still a developing field of study.[43]

In this study, a Langmuir film is utilized as a laboratory model for the surface of oceans, lakes, and atmospheric aerosol particles. Because of the diversity of the sources from which the atmospheric organics stem, mixed films are more appropriate than homogeneous monolayers, in order to better represent the complex composition of atmospheric aerosols.[1,9,44,45] Mixed films composed of surfactants with similar hydrophobic groups have been studied previously.[44,46] In this work, we chose a system composed of a soluble surfactant (L-phenylalanine) in conjunction with an insoluble surfactant (stearic acid), to monitor surface pressure induced morphological changes at the air−water interface in a mixed film. Here, two very different hydrophobic groups are utilized: L-phenylalanine has a bulky hydrophobic group composed of an aromatic ring, while stearic acid contains a long hydrocarbon chain as its hydrophobic group. The use of very different hydrophobic groups in a mixed film will add to the knowledge of the surface morphology of complex environmental interfaces such as the surface of atmospheric aerosols. Isotherm compression−expansion cycles were then utilized as a model for the complex dynamics at the ocean surface and processes that aerosol particles undergo throughout their atmospheric lifetime. In the atmosphere, the surface coverage of the aerosol particle may be changed through collision and subsequent coagulation of particles, as well as selective evaporation and uptake of water. Manually changing the surface area through the use of the trough's mechanical barriers mimics the compression and expansion the surface of the aerosol particles undergoes through these processes.

The choice of molecules used in this study is due to their atmospheric relevance and known surface activity. Stearic acid, as mentioned earlier, is one of the major surfactants found in atmospheric aerosols stemming from biogenic sources,[42] and forms a floating monolayer (solubility in water of only 0.0029 g/kg[47]) with well-known phase changes through induced surface pressure.[33] L-phenylalanine was chosen as it has one of the highest hydrophobicity ratings of the naturally occurring amino acids but is still soluble in water with a solubility of 27.9 g/kg, and has been previously seen to exhibit some surface activity.[48−50] Amino acids are also found in atmospheric aerosols,[51] and are known to participate in atmospheric processes.[52−54] The mixed film formed by deposited stearic acid with adsorbed L-phenylalanine at the air−water interface was studied using the Langmuir trough in conjunction with Brewster angle microscopy (BAM) and infrared reflection−absorption spectroscopy (IRRAS).

EXPERIMENTAL SECTION

Materials. All solvents and reagents were used without further purification. Stearic acid (octadecanoic acid, 98+%) was purchased from Aldrich Chemical Co., Inc. and then dissolved in chloroform (ACS grade, Mallinckrodt Baker, Inc.) to a concentration of 1 mg/mL. L-Phenylalanine (99%) was purchased from Alfa Aesar, and was prepared to a concentration of 0.02 M in distilled water (solution had a final pH of 6).

Instruments. *Langmuir Trough.* The Langmuir trough for isotherm studies was custom-built, and consists of a polytetrafluoroethylene (PTFE) trough (52 × 7 × 0.5 cm) coupled with two computer-controlled, PTFE barriers. The barriers were controlled using a computer interface and software purchased from NIMA (NIMA Technology Ltd., UK). The barriers were limited at their open position to an area of 300 cm^2, and at their closed position to an area of 30 cm^2 or surface pressure of 45 mN/m (whichever was reached first), with a constant barrier speed of 100 cm^2 min^{-1}.

The Langmuir trough for isotherm, BAM, and IRRAS studies was equipped with a Wilhelmy balance, which allowed for the measurement of surface pressure as the mechanical barriers were moved across the surface, with the measured area being the area between the moving mechanical barriers. This produces a surface pressure−area (π−A) isotherm, thereby giving interfacial thermodynamic information. In the experiments presented here, isotherm compression/expansion cycles were performed, during which the mechanical barriers continuously moved from their open to closed positions with constant barrier speed (with the limiting conditions described above).

Brewster Angle Microscope. A similar Langmuir trough as that described above (168 mm × 86 mm, KSV minitrough, Finland) was equipped with a custom-built BAM, which further allowed visualization of the air−water interface during the isotherm cycles.[55,56] The BAM experiments were carried out on a self-assembled symmetric goniometer system. The laser emits 5 mW p-polarized light at 543 nm (Research Electro-Optics, Inc.), which is incident at the Brewster angle of the subphase. The incident beam is passed through a Glen Thompson polarizer before reaching the liquid surface. An infinity-corrected 10° Nikon lens together with a tube lens are used to form the image. The BAM image is collected on an Andor back-illuminated electron-multiplier charge-coupled device (EMCCD; Andor DV887) of 512 × 512 pixels. In the BAM images shown here, the darkest (black) regions represent areas with negligible surfactant coverage (a two-dimensional (2D) gas phase), the medium gray areas indicate the presence of a condensed monomolecular film (e.g., of stearic acid), and very bright areas indicate the presence of three-dimensional (3D) structures (e.g., hydrophobic aggregates).

Infrared Reflection−Absorption Spectroscopy. IRRAS spectra were obtained using the external port of a Bruker Tensor 27 FTIR Spectrometer. The IR beam exited the FTIR spectrometer and was passed through a CaF_2 lens (remaining unpolarized), before being reflected off of two 2 in. gold mirrors positioned over a Langmuir trough, utilized to direct the IR beam onto the air-aqueous interface at an angle of 22° relative to the surface normal. This angle of incidence is within the optimum 0−40° found to be ideal for an air−aqueous interface and unpolarized light.[57] The reflected beam was then directed to a liquid nitrogen-cooled MCT detector. All external

optics and equipment were constantly purged with dry house air. Spectra were collected with a 1 cm^{-1} resolution and were averaged over 200 scans. A single channel spectrum of a bare water surface was used as the background spectrum. The IRRAS spectra presented here remain as reflectance-absorbance (RA) spectra, where RA = $-\log(R/R_o)$ with R being the IR reflectivity of the surface of interest, and R_o being the IR reflectivity of the bare water surface background. Such reflectivities are described using the Fresnel equations, whose details are presented elsewhere.[58] With unpolarized light incident at an angle of 22° relative to the surface normal of an air-aqueous interface as used here, the expected absorption bands will be negative.

Methods. *Isotherm Cycles.* The trough was initially filled with the desired subphase; either distilled water or 0.02 M L-phenylalanine in distilled water. Thirty microliters of stearic acid solution was then deposited dropwise on the surface with the barriers at the open position. The system was then allowed to equilibrate for 20 min (to allow for solvent evaporation and L-phenylalanine adsorption), after which 10 isotherm compression/expansion cycles were performed. BAM video of the interface was continuously obtained throughout this process, and still images were later extracted from the video. IRRAS spectra were also taken before and after the isotherm cycles (1 cm^{-1} resolution, averaged over 200 scans) with the barriers at their fully open position. The pH of the solution was unchanged throughout all experiments remaining at a pH of 6.

Adsorption. The Langmuir trough was filled with a 0.02 M solution of L-phenylalanine followed by the deposition of stearic acid as described above. The surface pressure was then monitored over time with the barriers in their fully open position (300 cm^2). As with the isotherm cycles, the BAM video of the interface was continuously recorded during the adsorption process.

RESULTS

In the following, complementary thermodynamic information from π–A isotherms was used in combination with structural information from BAM images and IRRAS spectra to develop a model regarding the behavior of the interfacial layer. All of these techniques are highly sensitive to surface films, and thereby give information about changes in orientation, packing density and morphology of the molecules residing at the air-aqueous interface. Stearic acid forms a very stable film with known thermodynamic features.[59] With negligible solubility[50] and vapor pressure,[60] stearic acid is unlikely to partition into the aqueous or gas phases, and remains primarily as a floating monolayer film. A typical π–A isotherm of a surfactant, such as the one shown in the inset of Figure 1a, exhibits features (such as plateaus and/or kinks) that indicate the presence of 2D phase transitions, representative of the ordering and interactions of the molecules at the surface.[61,62] Moving from large to small molecular area, the film begins in a 2D, disordered gaseous phase in which there is little order among the surfactant molecules at the surface, and the surface pressure is negligibly small. At smaller molecular area, a phase transition may be observed to a liquid expanded state in which there is some interaction among the surfactants but still some translational freedom. In the case of stearic acid, however, room temperature is below the triple point, and condensation to a liquid condensed phase occurs directly (at 24 $Å^2$ in the inset to Figure 1). A large number of studies using a variety of techniques have led to a deeper understanding of the various

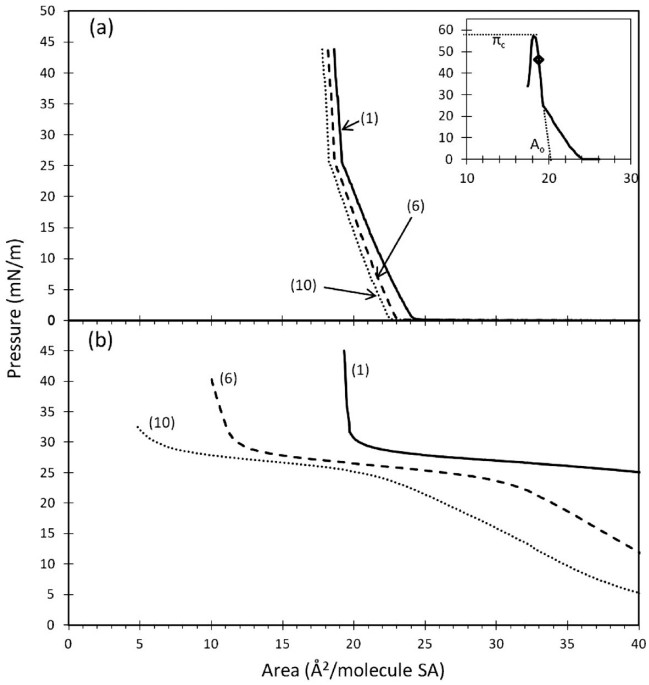

Figure 1. Isotherm compression cycle numbers 1, 6, and 10 of (a) stearic acid deposited on an aqueous subphase and (b) stearic acid deposited on an aqueous 0.02 M solution of L-phenylalanine. Inset shows a typical stearic acid isotherm on an aqueous subphase past the point of collapse, with the molecular footprint (A_o), collapse pressure (π_c), and maximum pressure for the isotherm cycles (◇) indicated.

fatty acid liquid condensed phases, which are now characterized as 2D liquid crystalline mesophases that vary in local packing geometry, molecular tilt, etc.[62−64] The molecules first pass through a tilted liquid condensed phase (seen at 24 $Å^2$ in the inset of Figure 1) where the surfactant tails are ordered at the surface with varying symmetries depending on the mesophase, but are tilted relative to the surface.[62,64] Then, if the barriers continue to close, another phase transition may occur to an untilted liquid condensed phase (~20 $Å^2$ in the inset to Figure 1) in which the surfactant molecules transition to occupying a minimum surface area. At even smaller molecular areas, the molecular monolayer becomes unstable with respect to collapse into a 3D interfacial layer. The nature of this collapse has been thoroughly studied and can vary depending on the film composition, the thermodynamic conditions, and the compression rate.[65,66] For example, some monolayers collapse via activated nucleation and growth of small 3D aggregates,[65,67,68] while others collapse via the formation of macroscopic "folds".[66] For stearic acid, the collapse pressure (π_c) is around 55 mN/m and is indicated by a sudden decrease in surface pressure, at which point complex 3D structures begin to form.[69] The regime of the isotherm corresponding to the untilted condensed phase is conventionally extrapolated to zero surface pressure to yield a characteristic molecular area, or footprint (A_o). The footprint for stearic acid is known to be ca. 20 $Å^2$/molecule.[69]

In the isotherms shown in Figure 1, the film was subjected to a series of compression/expansion cycles, of which only the compressions are shown. The film was not allowed to reach collapse, constrained to a maximum surface pressure of 45 mN/m. In Figure 1a, stearic acid alone was deposited on an aqueous subphase, while in Figure 1b, stearic acid was deposited on a

dx.doi.org/10.1021/jp303913e | J. Phys. Chem. B 2012, 116, 7849−7857

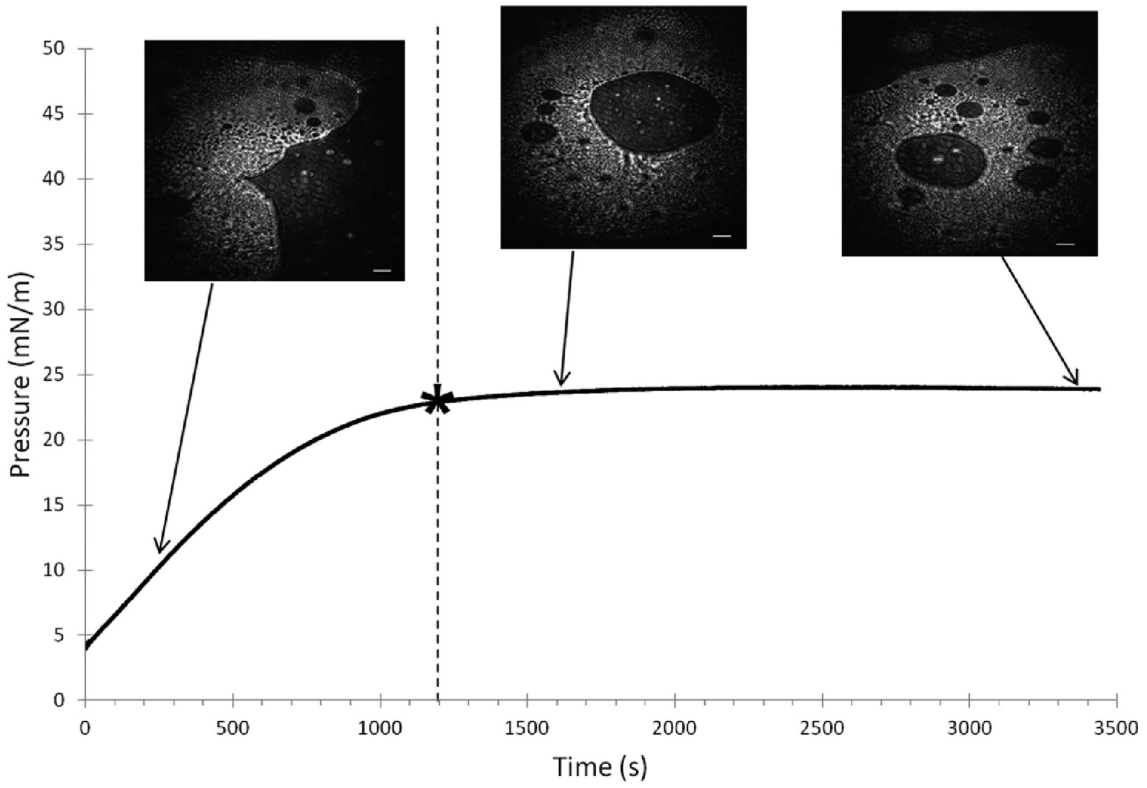

Figure 2. Surface pressure measured over time of 0.02 M L-phenylalanine solution after deposition of stearic acid with corresponding BAM images (scale bar representing 50 μm). The asterisk indicates the time at which the isotherm cycles were started in the experiments shown in Figures 1 and 3.

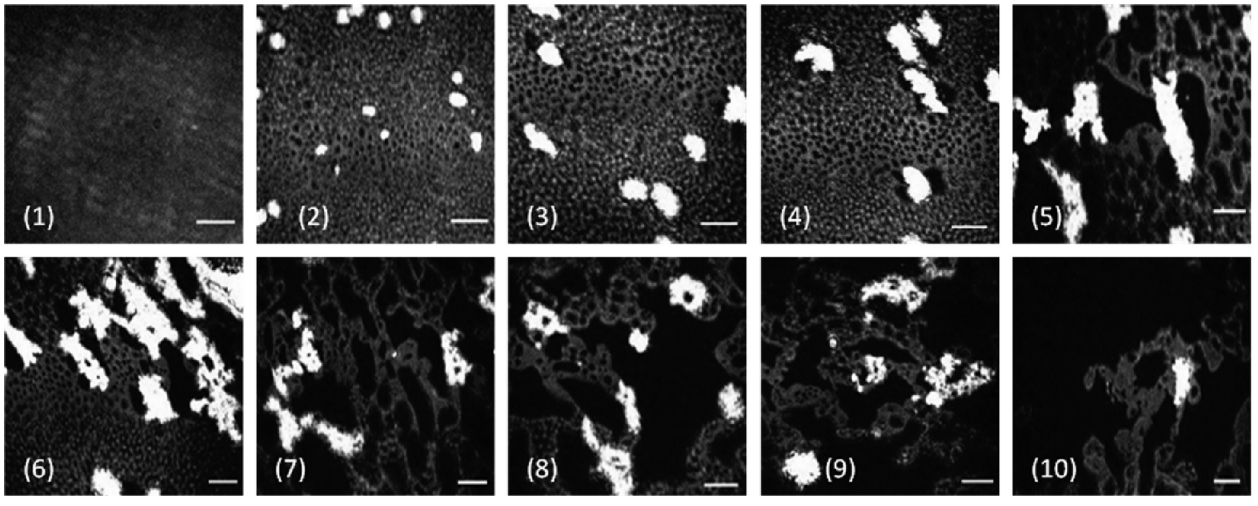

Figure 3. BAM images of stearic acid deposited on an aqueous 0.02 M solution of L-phenylalanine taken after compression to an area of 21 Å^2/molecule of stearic acid. Numbers 1−10 correspond to the isotherm cycle during which the image was taken with the scale bar representing 50 μm.

subphase composed of an aqueous solution of L-phenylalanine. Throughout the course of the isotherm cycles in Figure 1a, little loss of stearic acid was seen from the interface, evidenced by the small change in the footprint value (there was a decrease of ca. 1 Å^2/molecule throughout ten isotherm cycles). This is reinforced by BAM images of the stearic acid film alone (see Supporting Information, Figure S.1), which show that at a surface area of 21 Å^2/molecule in each cycle, there is simply a close-packed monolayer film with no evidence of any disruption or collapse structures. When an aqueous solution of L-phenylalanine is present prior to the deposition of stearic acid, however, the stearic acid film is modified (evidenced by the progressive decrease in the footprint presented in Figure 1b).

Phenylalanine is a soluble amino acid that partitions to some extent to the interface.[49] This surface partitioning is observed here as an increase in surface pressure over time as the molecule adsorbs to the air−water interface, a phenomenon which has been observed and characterized in other systems.[70] Figure 2 illustrates the change in surface pressure due to the adsorption of L-phenylalanine over time in the presence of a dilute stearic acid film. During this experiment, the stearic acid

dx.doi.org/10.1021/jp303913e | J. Phys. Chem. B 2012, 116, 7849−7857

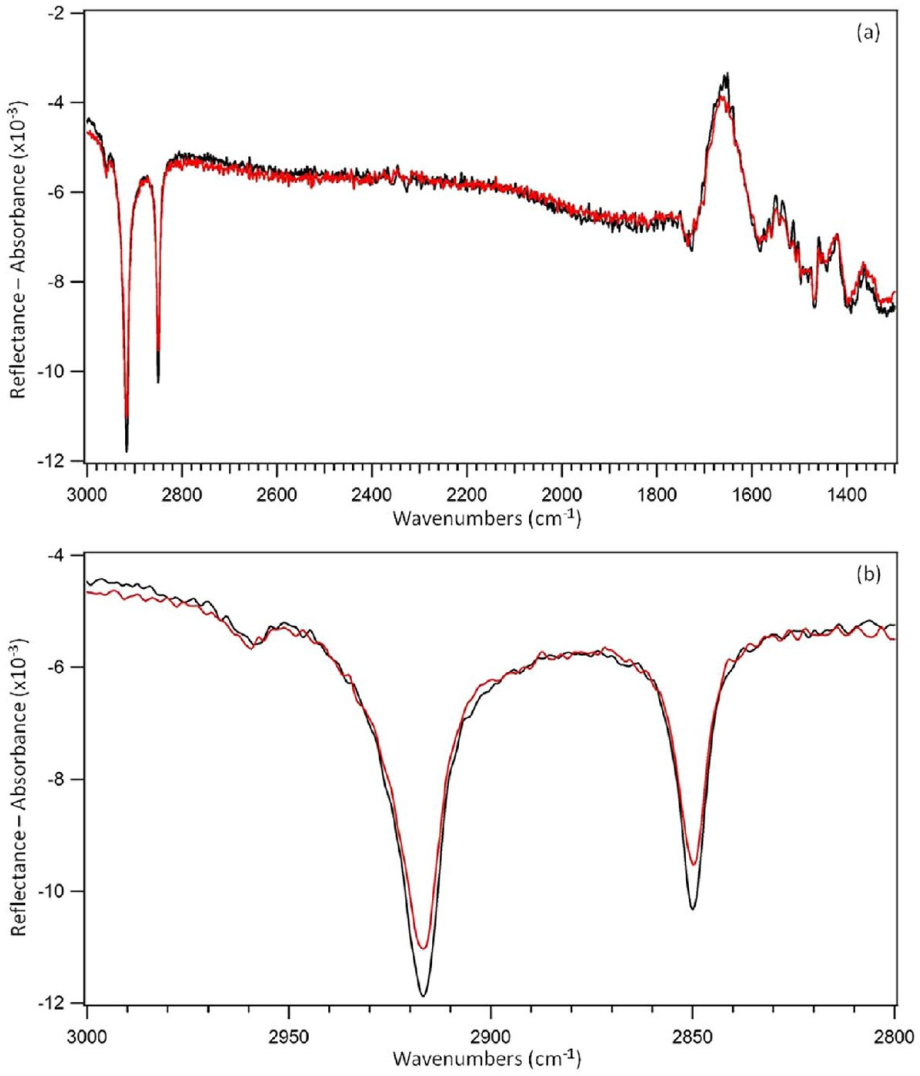

Figure 4. IRRAS spectra of the phenylalanine–stearic acid mixed film before isotherm cycles (black) and after isotherm cycles (red). The full IRRAS spectrum is shown in panel a, and only the C–H stretching region is shown in panel b.

monolayer was present at a molecular area of ~40 Å^2, conditions under which two-phase coexistence between a 2D gas and liquid condensed phase would be observed in the absence of a soluble surfactant. The asterisk and vertical broken line indicates the time at which the isotherm cycles were started in the experiment shown in Figures 1b and 3. The surface pressure ultimately reaches a maximum of 25 mN/m, at which point it remains constant for the duration of the adsorption experiment. The BAM images, indicated at varying points along the adsorption process of L-phenylalanine, suggest that a two-phase film is present throughout this adsorption process, with gray condensed phase regions appearing along with dark gas phase regions.

Thus, in Figure 1b, the increased surface pressure at large molecular areas can be attributed to the presence of adsorbed L-phenylalanine. However, at molecular areas approaching 20 Å^2 in the first isotherm cycle portrayed in Figure 1b, the isotherm appears to mirror that of a pure stearic acid monolayer. The footprint obtained through extending the stearic acid feature to zero surface pressure is consistent with the footprint of stearic acid on a bare aqueous subphase (Figure 1a). These observations are consistent with the removal (i.e., "squeezing out") of phenylalanine from the interface at surface pressures above ~30 mN/m. As the isotherm cycles progress, however, the stearic acid character diminishes evidenced by a progressively smaller footprint. This contrasts sharply with the behavior described earlier of a stearic acid film on a bare water subphase where very little loss in surfactant is seen throughout all 10 isotherm cycles. The experiments were also performed with a subphase containing a dilute (10^{-5} M) $CdSO_4$ solution to test the effect of salt content. It is well-known that divalent cations increase the stability of stearic acid monolayers.[71] However, the isotherm cycles performed on the system of stearic acid with an adsorbed phenylalanine film in the presence of Cd^{2+} resulted in the same loss of stearic acid character seen with a pure water subphase (see Supporting Information, Figure S.2). Again, in this experiment, the maximum surface pressure allowed was 45 mN/m, thereby avoiding monolayer collapse due to external barrier pressure. This indicates the modification of the otherwise stable stearic acid film due to the presence of the adsorbed L-phenylalanine. The modification was seen to persist over the course of at least 24 h, indicating that it was an irreversible change to the surface monolayer.

The disruption of the stearic acid film is visualized in the BAM images in Figure 3. This series of images was taken at an

dx.doi.org/10.1021/jp303913e | J. Phys. Chem. B 2012, 116, 7849–7857

area of 21 Å^2/molecule of stearic acid during each compression cycle. At this molecular area, the stearic acid film should be approaching its liquid condensed phase, with a close-packed, interacting monolayer. This area is also well below the collapse of the monolayer. In the image from the first cycle, all that can be seen is a close packed stearic acid film (seen as a fairly uniform gray color). There are no apparent holes or hydrophobic aggregates, as is to be expected from the isotherm data. As early as cycle 2, bright spots representing early collapse structures begin to appear. As the cycles progress, the collapse structures are more pronounced, begin to coalesce, and the surrounding monolayer film exhibits 2D phase coexistence of condensed and gaseous regions. These 2D gas phase regions become more prominent in the later cycles seen as large dark voids in the images.

The IRRAS spectra shown in Figure 4 also confirm the processing of the stearic acid film facilitated by phenylalanine. The spectrum shown in Figure 4a is the full spectrum of the stearic acid−phenylalanine mixed film before (black) and after 10 isotherm cycles (red) taken at a molecular area of 32 Å^2 of stearic acid. In this spectrum, it is clear that there is in fact a mixed film of stearic acid and phenylalanine in the surface region both before and after isotherm cycles, evidenced by the strong C−H stretch peaks around 2900 cm^{-1} due to the long hydrocarbon tail of stearic acid, as well as the weaker peaks below 1600 cm^{-1} due to phenylalanine (with the exception of the sharp peak at 1470 cm^{-1}, which is due to the CH_2 scissoring mode of stearic acid). It is also evident when comparing the IRRAS spectra both before and after isotherm cycles that there is no change in ionization state of either stearic acid or phenylalanine in the surface region, as there are no shifts or appearance/disappearance of any peaks in the full spectrum (Figure 4a). At the pH of 6 used in these studies, phenylalanine exists as a zwitterion. The carboxylic acid group of stearic acid has a bulk pK_a of ∼4.85, which increases to ∼8.7 at the surface, ensuring that at pH 6 the stearic acid molecules at the surface are un-ionized.[72,73] Thus, the effects seen here are not attributed to a change in the ionization state of the molecules at the surface.

When comparing the C−H stretch region before and after cycles, shown in Figure 4b, there is a decrease in intensity after the isotherm cycles. This decrease in intensity can be attributed to either less absorbing molecules in the illuminated surface area, or an orientational ordering change of the stearic acid molecules at the surface.[46,74] It is likely that both of these are contributing here, when this data is taken in conjunction with the BAM images shown in Figure 3. There is an orientational order change of the stearic acid hydrocarbon tails, seen in the BAM images by the formation of 3D aggregates throughout the cycles (bright spots in the images). There is also loss of stearic acid from the surface as seen by the large dark voids in the BAM images. Over the course of the isotherm cycles, the BAM images and IRRAS spectra reinforce the information gained from the isotherms themselves: that the presence of phenylalanine causes modification of the stearic acid film from a uniform hydrophobic surface to a heterogeneous surface containing 3D hydrophobic aggregates, regions of condensed monolayer, as well as exposed hydrophilic "holes" (2D gas).

DISCUSSION

Pure films of insoluble surfactants (such as stearic acid) are known to undergo the transition from a 2D film to form more complex 3D structures once a characteristic surface pressure has been reached and the film collapses.[66] Among the suggested collapse structures formed of single-component films are micelles that partition into the bulk aqueous phase, 3D aggregates that nucleate and grow at the interface, and the formation of bilayers and trilayers at the surface through film fracture followed by folding.[65−68] The formation of these collapse structures is often described as having a nucleation and growth mechanism, and has been visualized using BAM.[67,68,75] Mixed monolayers can have even more complex collapse mechanisms, depending on the components' miscibilities.[69,70,76−79] It is evident from the first isotherm cycle of the stearic acid/L-phenylalanine mixture (Figure 1b), that stearic acid and adsorbed L-phenylalanine form an immiscible mixed film. In a true miscible mixed film, there will only be one distinct collapse pressure that is usually different from that of either individual component.[69,76] In this case, there are two distinct collapse pressures, each characteristic of the individual components that point toward their existence at the surface as an immiscible mixed film.[69,76] This is seen as the "squeezing out" of L-phenylalanine, evidenced by the near-horizontal region of the isotherm at a surface pressure of ca. 25 mN/m, prior to the expected stearic acid liquid condensed phase.

The collapse of a monolayer to form soluble micelles may be envisioned through the tilting of adjacent surfactant molecules due to tail−tail interactions as described by Safran et al.[62,80] The heads are assumed to form an ordered array on the surface, while the hydrophobic tails are allowed to rotate. Safran et al. suggest that the mismatch between the size of the heads and tails of the surfactants promote the formation of "micellelike clusters", a deviation from the normal uniform tilt state. Here, there is either a larger head−head spacing than is preferred by the tail−tail interaction, or there is a larger tail−tail spacing than is preferred by the head−head interaction (resulting in the tails splaying outward from each other). The resultant structures are named "antisolitons" and "solitons" respectively. Safran et al. then concluded that the antisoliton state can be lower in energy than a uniform tilt state.[80] These antisoliton "micellelike clusters", when subjected to the external pressure supplied by the mechanical trough barriers, could fold on top of one another, forming a cluster of surfactants with hydrophilic heads on the outside and hydrophobic tails on the inside.

It is clear from the BAM images shown in Figure 3 that the collapse structures observed in this study are not folds resulting in multilayers (which would be seen as long, line-like structures),[66] nor are they micelles, which are nanometer-scale objects that would be invisible via BAM: micelles or larger hydrophilic aggregates would be soluble in the subphase, and would not remain at the surface in the plane of view. In fact, the structures that are formed during the compression cycles are consistent with macroscopic hydrophobic aggregates (i.e., particles) that remain at the interface, presumably due to their hydrophobic character.[81] This mechanism is consistent with recent work by Sierra-Hernandez and Allen showing aggregate formation of long chain halides on the surface of stearic and palmitic acid Langmuir films.[46] In order for such a structure to form, however, the tails of the surfactants must splay outward rather than bunch inward (comparable to Safran et al.'s soliton state versus antisoliton state[80]). This is generally considered to be a less favorable state (energetically) than either the state where the tails are bunched inward or a uniform tilt state. However, if a large hydrophobic group (like the phenyl ring from phenylalanine) is inserted between some of

these long hydrocarbon tails, it could force them to splay outward and begin the formation of these structures.

The stability and mechanism of the collapse of a monolayer is usually considered to be due to interactions among the head-groups of the surfactant molecules at the interface.[68,82] Through hydrogen bonding among the head-groups, stable bridging interactions are formed, and prevent the disruption of the ordering of the head-groups through collapse.[82,83] Hydrophobic interactions, however, may also be important in the formation of hydrophobic collapse structures at the interface. Hydrophobic interactions have been seen to disrupt stable hydrogen-bonded networks (like the network formed by the hydrophilic heads of the surfactant molecules) in previous studies.[84−86] Recently, Zangi et al. have used molecular dynamics simulations to propose a mechanism for the denaturing of proteins by urea, where the hydrophobic interaction between urea and the protein backbone is stronger than the interaction of water with the protein, thereby forcing its unfolding.[84] Chandler has more broadly explained hydrophobic phenomena that occur at interfaces as essentially water-excluding interactions, where a hydrophobic interaction is facilitated by the exclusion of water from between the hydrophobic regions along with the necessary disruption of hydrogen bonds at the interface.[87] Chen et al. have experimentally shown using BAM and sum-frequency spectroscopy that small soluble molecules such as dimethylsufloxide compete for the surface and can exclude water from the headgroup region, caging and prematurely condensing lipids.[86,88] In a system such as the one presented here, this disruption would be facilitated by the phenyl ring forcing its way in between the hydrocarbon tails and then, through a hydrophobic interaction, forcing the distortion of the monolayer. The hydrophilic head of the surfactant would still be able to form hydrogen bonds to the carboxylic acid and amine group on the amino acid, and the phenyl group would have been suspended above the surface as has been observed using sum-frequency spectroscopy,[49,89] allowing for the necessary hydrophobic interaction with the hydrocarbon tail. The resultant distortion would be manifested by the splaying of the long chains outward, and then through continued external pressure on the film, would force the formation of hydrophobic aggregates. In contrast to the micelles described earlier, these hydrophobic aggregates would remain at the surface, as was observed using BAM and confirmed by the continuing presence of stearic acid C−H stretches observed using IRRAS.

CONCLUSIONS

Surface films on atmospheric aerosols play an important role in chemistry and climate in both the prebiotic and contemporary atmospheres.[24,25,90,91] In the modern atmosphere, aerosols are known to have an effect on climate.[3] The aerosol direct effect (light attenuation) is significantly influenced by aerosol size, prompting the need for a better understanding of the hygroscopicity of the particles. Surfactants on aerosols have been proposed to impede the particles' ability to uptake water, thereby impeding its growth, but experiments present conflicting results. The aerosol indirect effect (ability to serve as cloud condensation nuclei) has also been suggested to be dependent upon the surface morphology of the particle through the dependence of Köhler theory on surface tension.[92] In this study we have shown that an otherwise stable surfactant film can be modified due to the presence of a soluble amino acid, exposing hydrophilic holes and forming hydrophobic aggregates at the air−water interface. This hydrophobic collapse suggests that the effect of surfactants on atmospheric aerosols is more complicated than a simple monolayer impeding water transfer. Instead, the composition of the entire aerosol and its atmospheric processing must be taken into consideration because molecules from the aerosol's interior may have the ability to significantly disrupt the surface morphology, thereby changing the surface tension of the particle (affecting its propensity to serve as a cloud condensation nucleus (CCN)) and possibly opening up hydrophilic holes to allow for increased water uptake and growth.

ASSOCIATED CONTENT

Supporting Information

BAM images of stearic acid only isotherm cycles and isotherms of L-phenylalanine−stearic acid mixed film in the presence of Cd^{2+} salt are presented as Supporting Information. This material is available free of charge via the Internet at http://pubs.acs.org.

AUTHOR INFORMATION

Corresponding Author

*E-mail: vaida@colorado.edu.

Notes

The authors declare no competing financial interest.

ACKNOWLEDGMENTS

V.V. and E.C.G. acknowledge funding from the National Science Foundation (NSF) CHE-1011770 for this work. E.C.G. acknowledges support from a NASA Earth and Space Science Fellowship. E.M.A. and H.C.A. acknowledge the NSF (CHE-1111762) for funding this project.

REFERENCES

(1) Finlayson-Pitts, B. J.; Pitts, J. N. *Chemistry of the Upper and Lower Atmosphere: Theory, Experiment, and Applications*; Academic Press: San Diego, 2000.

(2) Seinfeld, J. H.; Pandis, S. N. *Atmospheric Chemistry and Physics: From Air Pollution To Climate Change*; Wiley: New York, 1998.

(3) Solomon, S., Qin, D., Manning, M., Chen, Z., Marquis, M., Averyt, K. B., Tignor, M., Miller, H. L., Eds. *Climate Change 2007: The Physical Science Basis*; Contribution of Working Group I to the Fourth Assessment Report of the Intergovernmental Panel on Climate Change; Cambridge University Press: Cambridge, U.K., 2007.

(4) Jimenez, J. L.; Canagaratna, M. R.; Donahue, N. M.; Prevot, A. S. H.; Zhang, Q.; Kroll, J. H.; DeCarlo, P. F.; Allan, J. D.; Coe, H.; Ng, N. L.; et al. *Science* **2009**, *326* (5959), 1525−1529.

(5) Kanakidou, M.; Seinfeld, J. H.; Pandis, S. N.; Barnes, I.; Dentener, F. J.; Facchini, M. C.; Van Dingenen, R.; Ervens, B.; Nenes, A.; Nielsen, C. J.; et al. *Atmos. Chem. Phys.* **2005**, *5* (4), 1053−1123.

(6) Murphy, D. M.; Cziczo, D. J.; Froyd, K. D.; Hudson, P. K.; Matthew, B. M.; Middlebrook, A. M.; Peltier, R. E.; Sullivan, A.; Thomson, D. S.; Weber, R. J. *J. Geophys. Res., [Atmos.]* **2006**, *111* (D23), 15.

(7) Hallquist, M.; Wenger, J. C.; Baltensperger, U.; Rudich, Y.; Simpson, D.; Claeys, M.; Dommen, J.; Donahue, N. M.; George, C.; Goldstein, A. H.; et al. *Atmos. Chem. Phys.* **2009**, *9* (14), 5155−5236.

(8) Rudich, Y. *Chem. Rev.* **2003**, *103* (12), 5097−5124.

(9) Tervahattu, H.; Juhanoja, J.; Vaida, V.; Tuck, A. F.; Niemi, J. V.; Kupiainen, K.; Kulmala, M.; Vehkamaki, H. *J. Geophys. Res., [Atmos.]* **2005**, *110* (D6), 9.

(10) Tervahattu, H.; Juhanoja, J.; Kupiainen, K. *J. Geophys. Res., [Atmos.]* **2002**, *107* (D16), 4319.

(11) Facchini, M. C.; Mircea, M.; Fuzzi, S.; Charlson, R. J. *Nature* **1999**, *401* (6750), 257−259.

(12) Shulman, M. L.; Jacobson, M. C.; Carlson, R. J.; Synovec, R. E.; Young, T. E. *Geophys. Res. Lett.* **1996**, *23* (3), 277−280.
(13) Seidl, W. *Atmos. Environ.* **2000**, *34* (28), 4917−4932.
(14) Lang-Yona, N.; Abo-Riziq, A.; Erlick, C.; Segre, E.; Trainic, M.; Rudich, Y. *Phys. Chem. Chem. Phys.* **2010**, *12* (1), 21−31.
(15) Riziq, A. A.; Trainic, M.; Erlick, C.; Segre, E.; Rudich, Y. *Atmos. Chem. Phys.* **2008**, *8* (6), 1823−1833.
(16) Kwamena, N. O. A.; Buajarern, J.; Reid, J. P. *J. Phys. Chem. A* **2010**, *114* (18), 5787−5795.
(17) Hearn, J. D.; Smith, G. D. *Phys. Chem. Chem. Phys.* **2005**, *7* (13), 2549−2551.
(18) Fuzzi, S.; Andreae, M. O.; Huebert, B. J.; Kulmala, M.; Bond, T. C.; Boy, M.; Doherty, S. J.; Guenther, A.; Kanakidou, M.; Kawamura, K.; et al. *Atmos.c Chem. Phys.* **2006**, *6*, 2017−2038.
(19) Ellison, G. B.; Tuck, A. F.; Vaida, V. *J. Geophys. Res.* **1999**, *104* (D9), 11633−11641.
(20) Garland, R. M.; Wise, M. E.; Beaver, M. R.; DeWitt, H. L.; Aiken, A. C.; Jimenez, J. L.; Tolbert, M. A. *Atmos. Chem. Phys.* **2005**, *5*, 1951−1961.
(21) Wise, M. E.; Baustian, K. J.; Tolbert, M. A. *Proc. Natl. Acad. Sci. U.S.A.* **2010**, *107* (15), 6693−6698.
(22) Wise, M. E.; Garland, R. M.; Tolbert, M. A. *J. Geophys. Res., [Atmos.]* **2004**, *109* (D19), 14.
(23) Gill, P. S.; Graedel, T. E.; Weschler, C. J. *Rev. Geophys.* **1983**, *21* (4), 903−920.
(24) Dobson, C. M.; Ellison, G. B.; Tuck, A. F.; Vaida, V. *Proc. Natl. Acad. Sci. U.S.A.* **2000**, *97* (22), 11864−11868.
(25) Donaldson, D. J.; Vaida, V. *Chem. Rev.* **2006**, *106* (4), 1445−1461.
(26) Laurain, A. M. C.; Reid, J. P. *J. Phys. Chem. A* **2009**, *113* (25), 7039−7047.
(27) Rudich, Y.; Donahue, N. M.; Mentel, T. F. *Annu. Rev. Phys. Chem.* **2007**, *58* (1), 321−352.
(28) Reid, J. P.; Dennis-Smither, B. J.; Kwamena, N. O. A.; Miles, R. E. H.; Hanford, K. L.; Homer, C. J. *Phys. Chem. Chem. Phys.* **2011**, *13* (34), 15559−15572.
(29) Ziemann, P. J. *Nature* **2010**, *467*, 797−798.
(30) Tang, I. N. *J. Geophys. Res.* **1996**, *101* (D14), 19,245−19,250.
(31) Beaver, M. R.; Freedman, M. A.; Hasenkopf, C. A.; Tolbert, M. A. *J. Phys. Chem. A* **2010**, *114* (26), 7070−7076.
(32) Rideal, E. K. *J. Phys. Chem.* **1925**, *29*, 1585−1588.
(33) Gaines, G. L. *Insoluble Monolayers at Liquid-Gas Interfaces*; Interscience Publishers: New York, 1966.
(34) Langmuir, I.; Schaefer, V. J. *J. Franklin Inst.* **1943**, *235*, 119−162.
(35) Barnes, G. T. *Colloids Surf., A* **1997**, *126* (2−3), 149−158.
(36) Van Loon, L. L.; Minor, R. N.; Allen, H. C. *J. Phys. Chem. A* **2007**, *111* (31), 7338−7346.
(37) Torn, R. D.; Nathanson, G. M. *J. Phys. Chem. B* **2002**, *106* (33), 8064−8069.
(38) Lawrence, J. R.; Glass, S. V.; Nathanson, G. M. *J. Phys. Chem. A* **2005**, *109* (33), 7449−7457.
(39) Chen, Y.-Y.; Grace Lee, W.-M. *Chemosphere* **1999**, *38* (10), 2431−2448.
(40) Andrews, E.; Larson, S. M. *Environ. Sci. Technol.* **1993**, *27* (5), 857−865.
(41) Gilman, J. B.; Vaida, V. *J. Phys. Chem. A* **2006**, *110* (24), 7581−7587.
(42) Giddings, W. P.; Baker, M. B. *J. Atmos. Sci.* **1977**, *34* (12), 1957−1964.
(43) Wills, J. B.; Knox, K. J.; Reid, J. P. *Chem. Phys. Lett.* **2009**, *481* (4−6), 153−165.
(44) Gilman, J. B.; Tervahattu, H.; Vaida, V. *Atmos. Environ.* **2006**, *40* (34), 6606−6614.
(45) Djikaev, Y. S.; Donaldson, D. J. *J. Geophys. Res., [Atmos.]* **2001**, *106* (D13), 14447−14463.
(46) Sierra-Hernandez, M. R.; Allen, H. C. *Langmuir* **2010**, *26* (24), 18806−18816.
(47) Bagby, M. O., Carboxylix acids (survey). In *Kirk−Othmer Encyclopedia of Chemical Technology*, Kroschwitz, J. I., Howe-Grant, M., Eds.; Wiley: New York, 1993; Vol. *5*, pp 77−88.
(48) Bull, H. B.; Breese, K. *Arch. Biochem. Biophys.* **1974**, *161* (2), 665−670.
(49) Watry, M. R.; Richmond, G. L. *J. Phys. Chem. B* **2002**, *106* (48), 12517−12523.
(50) Lide, D. R., *Handbook of Chemistry and Physics*; CRC Press: Cleveland, OH, 2004.
(51) Matsumoto, K.; Uematsu, M. *Atmos. Environ.* **2005**, *39* (11), 2163−2170.
(52) Kristensson, A.; Rosenorn, T.; Bilde, M. *J. Phys. Chem. A* **2009**, *114* (1), 379−386.
(53) De Haan, D. O.; Corrigan, A. L.; Smith, K. W.; Stroik, D. R.; Turley, J. J.; Lee, F. E.; Tolbert, M. A.; Jimenez, J. L.; Cordova, K. E.; Ferrell, G. R. *Environ. Sci. Technol.* **2009**, *43* (8), 2818−2824.
(54) Noziere, B.; Cordova, A. *J. Phys. Chem. A* **2008**, *112* (13), 2827−2837.
(55) Henon, S.; Meunier, J. *Rev. Sci. Instrum.* **1991**, *62* (4), 936−939.
(56) Honig, D.; Mobius, D. *J. Phys. Chem.* **1991**, *95* (12), 4590−4592.
(57) Dluhy, R. A. *J. Phys. Chem.* **1986**, *90* (7), 1373−1379.
(58) Gericke, A.; Michailov, A. V.; Hühnerfuss, H. *Vib. Spectrosc.* **1993**, *4* (3), 335−348.
(59) Gilman, J. B.; Eliason, T. L.; Fast, A.; Vaida, V. *J. Colloid Interface Sci.* **2004**, *280* (1), 234−243.
(60) Yaws, C. L. *Handbook of Vapor Pressure*; Gulf Pub: Houston, 1994.
(61) Knobler, C. M.; Desai, R. C. *Annu. Rev. Phys. Chem.* **1992**, *43*, 207−236.
(62) Kaganer, V. M.; Mohwald, H.; Dutta, P. *Rev. Mod. Phys.* **1999**, *71* (3), 779−819.
(63) Riviere, S.; Henon, S.; Meunier, J.; Schwartz, D. K.; Tsao, M. W.; Knobler, C. M. *J. Chem. Phys.* **1994**, *101* (11), 10045−10051.
(64) Kaganer, V. M.; Peterson, I. R.; Kenn, R. M.; Shih, M. C.; Durbin, M.; Dutta, P. *J. Chem. Phys.* **1995**, *102* (23), 9412−9422.
(65) Smith, R. D.; Berg, J. C. *J. Colloid Interface Sci.* **1980**, *74* (1), 273−286.
(66) Ybert, C.; Lu, W.; Möller, G.; Knobler, C. M. *J. Phys. Chem. B* **2002**, *106* (8), 2004−2008.
(67) Vollhardt, D. *Adv. Colloid Interface Sci.* **2006**, *123−126*, 173−188.
(68) Angelova, A.; Vollhardt, D.; Ionov, R. *J. Phys. Chem.* **1996**, *100* (25), 10710−10720.
(69) Roberts, G. *Langmuir−Blodgett Films*; Plenum Press: New York, 1990.
(70) Lee, Y. L.; Lin, J. Y.; Lee, S. *Langmuir* **2007**, *23* (4), 2042−2051.
(71) Yazdanian, M.; Yu, H.; Zografi, G.; Kim, M. W. *Langmuir* **1992**, *8* (2), 630−636.
(72) Miranda, P. B.; Du, Q.; Shen, Y. R. *Chem. Phys. Lett.* **1998**, *286* (1−2), 1−8.
(73) Tang, C. Y.; Huang, Z. S. A.; Allen, H. C. *J. Phys. Chem. B* **2010**, *114* (51), 17068−17076.
(74) Mitchell, M. L.; Dluhy, R. A. *J. Am. Chem. Soc.* **1988**, *110* (3), 712−718.
(75) Siegel, S.; Honig, D.; Vollhardt, D.; Mobius, D. *J. Phys. Chem.* **1992**, *96* (20), 8157−8160.
(76) Phillips, M. C.; Joos, P. *Kolloid-Z. Z. Polym.* **1970**, *238* (1−2), 499.
(77) Seoane, R.; Minones, J.; Conde, O.; Casas, M.; Iribarnegaray, E. *J. Phys. Chem. B* **2000**, *104* (32), 7735−7744.
(78) Teixeira, A. C. T.; Fernandes, A. C.; Garcia, A. R.; Ilharco, L. M.; Brogueira, P.; da Silva, A. *Chem. Phys. Lipids* **2007**, *149* (1−2), 1−13.
(79) Ocko, B. M.; Kelley, M. S.; Nikova, A. T.; Schwartz, D. K. *Langmuir* **2002**, *18* (25), 9810−9815.
(80) Safran, S. A.; Robbins, M. O.; Garoff, S. *Phys. Rev. A* **1986**, *33* (3), 2186−2189.
(81) Levinger, N. E.; Swafford, L. A. *Annu. Rev. Phys. Chem.* **2009**, *60*, 385−406.

(82) Lee, K. Y. C. *Annu. Rev. Phys. Chem.* **2008**, *59*, 771−791.
(83) Ries, H. E. *Nature* **1979**, *281* (5729), 287−289.
(84) Zangi, R.; Zhou, R. H.; Berne, B. J. *J. Am. Chem. Soc.* **2009**, *131* (4), 1535−1541.
(85) Hua, L.; Zangi, R.; Berne, B. J. *J. Phys. Chem. C* **2009**, *113* (13), 5244−5253.
(86) Chen, X. K.; Huang, Z. S.; Hua, W.; Castada, H.; Allen, H. C. *Langmuir* **2010**, *26* (24), 18902−18908.
(87) Chandler, D. *Nature* **2002**, *417* (6888), 491−491.
(88) Chen, X.; Allen, H. C. *J. Phys. Chem. A* **2009**, *113* (45), 12655−12662.
(89) Shultz, M. J.; Baldelli, S.; Schnitzer, C.; Simonelli, D. *J. Phys. Chem. B* **2002**, *106* (21), 5313−5324.
(90) Donaldson, D. J.; Tervahattu, H.; Tuck, A. F.; Vaida, V. *Origins Life Evol. Biospheres* **2004**, *34* (1−2), 57−67.
(91) Ruiz-Bermejo, M.; Menor-Salvan, C.; Osuna-Esteban, S.; Veintemillas-Verdaguer, S. *Origins Life Evol. Biospheres* **2007**, *37* (2), 123−142.
(92) Sorjamaa, R.; Svenningsson, B.; Raatikainen, T.; Henning, S.; Bilde, M.; Laaksonen, A. *Atmos. Chem. Phys.* **2004**, *4*, 2107−2117.